Quantum Monte Carlo method applied to non-Markovian barrier transmission

Guillaume Hupin and Denis Lacroix
Grand Accélérateur National d'Ions Lourds, Boulevard Henri Becquerel, Boîte Postale 55027, F-14076 Caen CEDEX 5, France
(Received 9 July 2009; revised manuscript received 25 September 2009; published 21 January 2010)

In nuclear fusion and fission, fluctuation and dissipation arise because of the coupling of collective degrees of freedom with internal excitations. Close to the barrier, quantum, statistical, and non-Markovian effects are expected to be important. In this work, a new approach based on quantum Monte Carlo addressing this problem is presented. The exact dynamics of a system coupled to an environment is replaced by a set of stochastic evolutions of the system density. The quantum Monte Carlo method is applied to systems with quadratic potentials. In all ranges of temperature and coupling, the stochastic method matches the exact evolution, showing that non-Markovian effects can be simulated accurately. A comparison with other theories, such as Nakajima-Zwanzig or time-convolutionless, shows that only the latter can be competitive if the expansion in terms of coupling constant is made at least to fourth order. A systematic study of the inverted parabola case is made at different temperatures and coupling constants. The asymptotic passing probability is estimated by different approaches including the Markovian limit. Large differences with an exact result are seen in the latter case or when only second order in the coupling strength is considered, as is generally assumed in nuclear transport models. In contrast, if fourth order in the coupling or quantum Monte Carlo method is used, a perfect agreement is obtained.

DOI: 10.1103/PhysRevC.81.014609 PACS number(s): 24.60.−k, 25.70.Jj, 05.60.Gg

I. INTRODUCTION

To understand nuclear reactions, the dynamics of nuclei is often replaced by few selected collective degrees of freedom expected to contain important information on the dynamic. This is, for instance, the case in fusion reactions where the relative distance and/or mass asymmetry are retained [1,2]. Another example is provided by the fission process, which is often treated as a trajectory in an energy landscape function on different deformation parameters [3,4]. Although the evolution is projected onto few variables, other internal degrees of freedom may play an important role in understanding the onset of dissipation or fluctuation phenomena [5]. To treat these effects, the relevant degrees of freedom should be regarded as an open quantum system (OQS) coupled to an environment that simulates the internal dynamics.

To include dissipation in collective space, two important simplifications are often made. First, most current models treating fusion/fission neglect quantum effects and consider a classical treatment [6–9]. Such an approximation is, however, expected to be valid only if the internal excitation is high and therefore is not expected to hold close to or below the Coulomb barrier. As discussed in Ref. [10], a proper treatment of quantum and decoherence effects might be crucial in this region. Second, when the timescale associated with collective dynamics cannot be dissociated from the timescale of the environment, the "non-Markovian" (also called "memory") effect should also be properly treated [11,12]. Great effort is now devoted to accounting for both quantal and non-Markovian effects in nuclear reactions [13–18] and, more generally, in OQSs [19].

Recently, the description of OQSs by stochastic methods has received much attention [19–21]. In the Markovian limit, several methods have been proposed to treat fluctuation and dissipation starting from a quantum master equation of the system density [19,20,22–28]. These methods have been extended also to treat non-Markovian effects, such as in quantum state diffusion (QSD) [29–32] or quantum Monte Carlo (QMC) methods [33]. Several groups have shown that these effects could eventually be simulated using a Feynman-Vernon influence functional [21,34] or directly stochastic master equations [35,36].

In this article, we apply the stochastic formulation proposed in Ref. [36] to the case of quadratic potentials coupled to a heat bath: the so-called Caldeira-Leggett (CL) model [37]. The case of inverted potential is the first step toward realistic situations like fusion or fission. The aim of this article is threefold: first, to introduce the new QMC method and apply it to potentials with barriers similar to those appearing in fusion/fission processes; second, to show that the exact QMC method can be rather accurate in treating the dissipative dynamics of a quantum system; and last, to present a comparison of this theory with other methods based on projection, namely, Nakajima-Zwangig (NZ) and time-convolutionless (TCL) [38–41], which are actually widely used to treat non-Markovian effects. Doing so, we show that only TCL up to at least fourth order in the coupling constant can provide a competitive theory. The article is organized as follows. In Sec. II, the ingredients and properties of the QMC approach are discussed, and the link with a functional integral is precisely determined. In Sec. III, the method is first illustrated for the case of a parabolic potential. Then, the passing probabilities are estimated for the inverted parabola case.

II. QMC METHOD

Our starting point is a system (S) interacting with a surrounding environment (E). We assume here that the total system ($S + E$) is described by the Hamiltonian

$$H = H_S + H_E + V. \quad (1)$$

H_S (H_E) acts on the system (environment) only while V induces a coupling between the two subsystems. Starting from an initial total density $D(0)$, the dynamical evolution is given by the Liouville-von Neumann equation on the density:

$$i\hbar\frac{dD(t)}{dt} = [H, D(t)]. \tag{2}$$

In many physical situations, the total number of degrees of freedom to follow in time prevents from solving this equation exactly. One of the leitmotifs of OQS theory is to find accurate approximations for the system evolution without following explicitly irrelevant degrees of freedom associated with the environment, therefore reducing the complexity of the initial problem. A conventional strategy to treat dissipation and fluctuation in an OQS is to reduce the information to the system density only, $\rho_S(t) = \mathrm{Tr}_E(D(t))$, while accounting approximately for the environment effect. Here we use a different strategy: The dynamics of the total system is first replaced by a set of stochastic evolutions where the total density remains separable along each path, that is, $D = \rho_S(t) \otimes \rho_E(t)$. Then, the stochastic evolution of the environment is projected onto the relevant degrees of freedom to obtain a closed equation for the system density. It is shown that the new approach provides a proper treatment of dissipation and fluctuation for a system coupled to a surrounding heat bath.

A. QMC formulation of OQSs

Recently, new stochastic formulations [34,35,42,43] have been developed to study the $S + E$ problem that avoid evaluation of nonlocal memory kernels, although non-Markovian effects are accounted for exactly (see also [35,36,42,44–47]). One example of such a theory based on the QMC method is presented here.

Hereafter, it is assumed that the coupling is separable: $V = Q \otimes B$, where Q and B act on the system and environment, respectively. For simplicity, an initial separable density is considered, that is, $D(0) = \rho_S(0) \otimes \rho_E(0)$. We want to replace the evolution of the total density [Eq. (2)] by an ensemble of stochastic evolutions of both the system and environment such that

$$\begin{cases} d\rho_S = \frac{dt}{i\hbar}[H_S, \rho_S] + d\xi_S Q\rho_S + d\lambda_S \rho_S Q, \\ d\rho_E = \frac{dt}{i\hbar}[H_E, \rho_E] + d\xi_E B\rho_E + d\lambda_E \rho_E B, \end{cases} \tag{3}$$

where $d\xi_{S/E}$ and $d\lambda_{S/E}$ denote Markovian Gaussian stochastic variables with zero means and where we use the Ito convention of stochastic calculus [48]. In the following, we assume, in addition, that

$$\overline{d\xi_S d\lambda_E} = \overline{d\lambda_S d\xi_E} = 0, \tag{4}$$

where the overline denotes the stochastic average. Along each path, the total density remains separable, that is, $D(t) = \rho_S(t) \otimes \rho_E(t)$. Starting from such a density, at time $t + dt$, the average evolution deduced from Eq. (3) is given by

$$\overline{dD(t)} = \frac{dt}{i\hbar}[h_S + h_E, D(t)] + \overline{d\xi_S d\xi_E}(Q \otimes B)D(t) + \overline{d\lambda_S d\lambda_E} D(t)(Q \otimes B).$$

Therefore, under the conditions

$$\overline{d\xi_S d\xi_E} = \frac{dt}{i\hbar}, \quad \overline{d\lambda_S d\lambda_E} = -\frac{dt}{i\hbar}, \tag{5}$$

the average evolution over the separable densities that evolve according to Eq. (3) identifies with the exact Liouville-von Neumann equation of motion [Eq. (2)]. The possibility of using simple Gaussian noises to incorporate the environment effect might appear surprising. Indeed, noises used in standard approaches for OQSs generally reflect properties of the environment. It should, however, be kept in mind that such environment-dependent noises appear once the environment dynamics has been projected on the system density evolution. Anticipating the discussion of Sec. II B, once such a projection has been made, the Gaussian noises introduced here transform into new random variables that explicitly depend on the environment properties.

The preceding discussion for one time step can then be iterated to show that the exact dynamics of a $S + E$ problem could be replaced by an average over an ensemble of stochastic evolutions of separable densities [34–36]. To be really useful, mainly, two difficulties should be overcome: (i) In general, the environment corresponds to a large number of degrees of freedom that could not be followed explicitly in time and (ii) the numerical implementation of such a theory is possible only if the statistical errors do not grow too fast during the time evolution. These statistical errors are directly connected to the number of trajectories necessary to accurately describe the physical process. The first difficulty is solved in the next section by projecting the effect of the environment on the system, leading to a closed equation for the system density only. Let us first concentrate on statistical errors. At any time, a measure of the statistical fluctuation around the average trajectory is given by

$$\begin{aligned} \Lambda_{\mathrm{stat}} &= \overline{\mathrm{Tr}\{(D^\dagger(t) - \overline{D^\dagger(t)})(D(t) - \overline{D(t)})\}} \\ &= \overline{\mathrm{Tr}\{D^\dagger D(t)\}} - \mathrm{Tr}\{\overline{D(t)}^2\}. \end{aligned} \tag{6}$$

Starting from Eq. (3), the evolution of Λ_{stat} over a small time step reads

$$d\Lambda_{\mathrm{stat}} = \frac{2dt}{\hbar}\{\overline{\langle Q^2\rangle_S} + \overline{\langle B^2\rangle_E}\}, \tag{7}$$

where $\langle Q^2\rangle_S \equiv \mathrm{Tr}_S(Q^2\rho_S(t))$ and $\langle B^2\rangle_E \equiv \mathrm{Tr}_E(B^2\rho_E(t))$. Statistical errors associated with Eq. (3) have been estimated numerically and turn out to grow very fast in time [46]. As a consequence, the stochastic process in the present form is useless for simulating physical situations, and methods to reduce statistical errors should be used.

To do so, it is worth noting that the stochastic equation of motion is not unique. Indeed, any stochastic process of the form

$$\begin{cases} d\rho_S = \frac{dt}{i\hbar}[H_S + Q\Delta_E, \rho_S], \\ \qquad + d\xi_S(Q - \Delta_S)\rho_S + d\lambda_S, \rho_S(Q - \Delta_S) \\ d\rho_E = \frac{dt}{i\hbar}[H_E + B\Delta_S, \rho_E], \\ \qquad + d\xi_E(B - \Delta_E)\rho_E + d\lambda_E \rho_E(B - \Delta_E), \end{cases} \tag{8}$$

where $\Delta_S(t)$ and $\Delta_E(t)$ are time-dependent parameters, leads to the same average evolution. These stochastic equations also

provide a reformulation of the initial $S + E$ problem. Indeed, we have

$$\overline{d\rho_S \otimes \rho_E} + \overline{\rho_S \otimes d\rho_E} = \frac{dt}{i\hbar}[H_S + Q\Delta_E, \rho_S \otimes \rho_E] + \frac{dt}{i\hbar}[H_E + B\Delta_S, \rho_S \otimes \rho_E],$$

$$\overline{d\rho_S \otimes d\rho_E} = \frac{dt}{i\hbar}[(Q - \Delta_S) \otimes (B - \Delta_E), \rho_S \otimes \rho_E].$$

Therefore terms appearing in the deterministic part are exactly compensated by equivalent terms coming from the average over the noise. Accordingly, the evolution of the average density identifies with the exact equation of motion [Eq. (2)].

Up to now, the flexibility has been essentially exploited by using [35,36]

$$\Delta_E(t) = \langle B(t)\rangle_E, \Delta_S(t) = \langle Q(t)\rangle_S. \tag{9}$$

This choice is justified by the fact that it directly appears when the Ehrenfest theorem is applied to separable total density for system or environment observables. By modifying the stochastic evolution, part of the coupling is already contained in the deterministic evolution. Accordingly, we do expect that the amount of coupling to be treated by the noise is significantly reduced, as are the statistical errors. In the latter case, statistical fluctuations are given by

$$d\Lambda_{\text{stat}} = \frac{2dt}{\hbar}\{\overline{(\langle Q^2\rangle_S - \overline{\langle Q\rangle_S}^2)} + \overline{(\langle B^2\rangle_S - \overline{\langle B\rangle_S}^2)}\} \tag{10}$$

and are always smaller than the original ones [Eq. (7)]. As shown numerically in Ref. [35], Eq. (9) significantly reduces statistical fluctuations and opens new perspectives for the application of the present framework.

The modified stochastic theory has other advantages. For instance, the traces of densities are constant and remain equal to their initial values, that is, $d\text{Tr}(\rho_{S/E}) = 0$. This greatly simplifies expectation values of system and/or environment observables. Indeed, denoting by X a system operator, along a trajectory, we have

$$\langle X\rangle = \text{Tr}_E(XD(t)) = \text{Tr}(\rho_E(t))\text{Tr}_S(X\rho_S(t)). \tag{11}$$

For stochastic processes with varying traces of densities, the observable evolution will contain terms coming from $d\text{Tr}(\rho_{S/E})$ and cross-terms coming from $d\text{Tr}(\rho_{S/E})$ $d\text{Tr}(X\rho_S(t))$. In the case considered here, we simply have

$$d\langle X\rangle = \text{Tr}_E(\rho_E(t))d\text{Tr}_S(X\rho_S(t)). \tag{12}$$

The QMC theory with centered noise overcomes the second difficulty given earlier but does not help for the first difficulty because the environment degrees of freedom should still be followed in time. In the next section, we show how irrelevant degrees of freedom can be projected out to obtain a closed stochastic master equation for the system only.

B. Reduced system density evolution and link with influence-functional theory

The stochastic formulation suffers a priori from the same difficulty as the total dynamics: The environment is, in general, rather complex and has a large number of degrees of freedom, which can hardly be followed in time. In Eq. (8), the influence of the environment on the system only enters through $\langle B(t)\rangle_E$. Therefore, instead of following the full environment density evolution, one can concentrate on this observable only. As shown in Ref. [43], the second equation in Eq. (8) can be integrated in time to give

$$\langle B(t)\rangle_E = \text{Tr}_E(B^I(t - t_0)\rho_E(t_0)) - \frac{1}{\hbar}\int_0^t D(t,s)\langle Q(s)\rangle_S ds - \int_0^t D(t,s)du_E(s) + \int_0^t D_1(t,s)dv_E(s), \tag{13}$$

where B^I denotes the operator B written in the interaction picture, while D and D_1 are the memory function given by

$$D(t,s) \equiv i\langle[B(t), B(t-s)]\rangle_E, \quad D_1(t,s) \equiv \langle\{B(t), B(t-s)\}\rangle_E - 2\langle B(t)\rangle_E\langle B(t-s)\rangle_E. \tag{14}$$

A new set of stochastic variables $dv_{S/E}$ and $du_{S/E}$ have been introduced through $d\xi_{S/E} = dv_{S/E} - idu_{S/E}$ and $d\lambda_{S/E} = dv_{S/E} + idu_{S/E}$ and verify

$$\overline{du_S du_E} = \overline{dv_S dv_E} = \frac{dt}{2\hbar}, \overline{du_S dv_E} = \overline{dv_S du_E} = 0. \tag{15}$$

Reporting the evolution of $\langle B(t)\rangle_E$ into the evolution of ρ_S, a closed stochastic equation of motion for the system density is obtained:

$$d\rho_S = \frac{dt}{i\hbar}[H_S, \rho_S] + dt[Q, \rho_S]\int_0^t ds D(t-s)\langle Q(s)\rangle_S + d\xi(t)[Q, \rho_S] + d\eta(t)\{Q - \langle Q\rangle_S, \rho_S\}, \tag{16}$$

with

$$d\xi(t) = dt\int_0^t D_1(t-s)dv_E(s) - dt\int_0^t D(t-s)du_E(s) - idv_S(t), \quad d\eta(t) = du_S(t). \tag{17}$$

By integrating out the evolution of the environment, a new stochastic term is found that depends not only on the noise at time t, but also on its full history through the time integrals. Using second moments given by Eqs. (15) leads to

$$\overline{d\eta(t)d\eta(t')} = 0,$$
$$\overline{d\xi(t)d\eta(t')} = -\frac{dt}{2\hbar}\Theta(t-t')D(t-t'),$$
$$\overline{d\xi(t)d\xi(t')} = -\frac{idt}{2\hbar}D_1(|t-t'|),$$

where $\Theta(t - t') = 1$ if $t > t'$, and 0 elsewhere. Interestingly enough, the stochastic equation given by Eq. (16) identifies with the stochastic master equation obtained in Ref. [21] using a completely different method based on the Feynman-Vernon influence functional theory [49]. It should, however, be kept in mind that different strategies to design the stochastic equation (see the discussion in Sec. II A) would have given a different stochastic master equation.

Despite the apparent complexity of Eq. (16), the QMC approach has been recently applied with success to the spin-boson model coupled to a heat bath of oscillators [43]. In particular, the introduction of Eq. (9) seems to cure the

numerical difficulties that have been encountered in this model [46]. By projecting the environment effect onto the system density evolution, we no longer need to follow the environment density, and we expect that a rather limited number of trajectories will be sufficient to accurately simulate the onset of dissipation and fluctuation in an OQS. Equation (16) is the equation that is solved in practice. It should be noted that the present stochastic process differs significantly from conventional approaches. Indeed, according to the noise properties, system densities are non-Hermitian along a stochastic path. As a consequence, the expectation values of observables are complex, losing their physical meaning before averaging over the stochastic path. Nevertheless, we illustrate in the following that the new theory can be a very powerful tool.

III. APPLICATIONS

The CL model [37] corresponds to a single harmonic oscillator coupled to an environment of harmonic oscillators initially at thermal equilibrium, that is,

$$H_S = H_c + \frac{P^2}{2M} + \varepsilon\frac{1}{2}M\omega_0^2 Q^2, \tag{18}$$

$$H_E = \sum_n \left(\frac{p_n^2}{2m_n} + \frac{1}{2}m_n\omega_n^2 x_n^2\right), \tag{19}$$

and $B \equiv -\sum_n \kappa_n x_n$ [19]. Here $H_c = Q^2\sum_n \frac{\kappa_n^2}{2m_n\omega_n^2}$ is the counterterm that ensures that the physical frequency is ω_0. In the following, ε is either $+1$ (harmonic case) or -1 (inverted parabola case). Such a model can be solved exactly.

As shown in Ref. [43], the two functions D and D_1 defined by Eqs. (15) and estimated along the stochastic trajectories identify with the standard time correlation functions:

$$D(\tau) = 2\hbar\int_0^{+\infty} d\omega J(\omega)\sin(\omega\tau), \tag{20}$$

$$D_1(\tau) = 2\hbar\int_0^{+\infty} d\omega J(\omega)\coth(\hbar\omega/2k_BT)\cos(\omega\tau), \tag{21}$$

where $J(\omega) \equiv \sum_n(\kappa_n^2/2m_n\omega_n)\delta(\omega-\omega_n)$ denotes the spectral density characteristic of the environment [19,50]. In the following, a Drude spectral density [43],

$$J(\omega) = \frac{2M\eta}{\pi}\omega\frac{\Omega^2}{\omega^2+\Omega^2}, \tag{22}$$

is considered, where M is the nucleon mass.

A. QMC method for parabolic potentials

As a first illustration, the harmonic case ($\varepsilon = +1$) is considered. This case has been already studied in Ref. [51] using the stochastic method proposed in Ref. [21]. In the CL model, starting from an initial Gaussian density, the system density remains Gaussian along the stochastic path. Therefore the stochastic evolution of the system density reduces to the first and second moment evolution of $\langle P\rangle$ and $\langle Q\rangle$, given by [36]

$$\begin{cases} d\langle Q\rangle &= \frac{\langle P\rangle}{M}dt + 2du_S\sigma_{QQ}, \\ d\langle P\rangle &= -M\omega_0^2\langle Q\rangle dt - dt\langle B\rangle + 2du_S\sigma_{PQ} - \hbar dv_S, \\ d\sigma_{QQ} &= 2\frac{dt}{M}\sigma_{PQ}, \\ d\sigma_{PP} &= -2M\omega_0^2 dt\sigma_{PQ}, \\ d\sigma_{PQ} &= \frac{dt}{M}\sigma_{PP} - M\omega_0^2\sigma_{QQ}dt. \end{cases} \tag{23}$$

These equations illustrate the differences between the new exact reformulation and standard methods to treat dissipation. Generally, the noise enters into the evolution of $\langle P\rangle$ only and affects directly the second moment. Here we see that second moments identify with the unperturbed ones, while the random forces enter in both $\langle Q\rangle$ and $\langle P\rangle$. In addition, the noise is complex, which implies that observables make excursions into the complex plane. This stems from the specific noise used to design the exact formulation that leads to non-Hermitian densities along paths. Part of the conceptual difficulty in understanding the physical meaning of observable evolutions can be overcome by noting that if $\rho_S(t)$ belongs to the set of trajectories, by symmetry, $\rho_S^\dagger(t)$ will also belong to the set. By grouping these two trajectories to estimate observables, real quantities are deduced.

The exact evolution is obtained by averaging over different trajectories. For second moments, this leads to

$$\Sigma_{QQ} \equiv \overline{\langle Q^2\rangle} - \overline{\langle Q\rangle}^2 = \sigma_{QQ} + \overline{\langle Q\rangle^2} - \overline{\langle Q\rangle}^2, \tag{24}$$

where $\overline{\langle X\rangle}$ denotes the statistical average of quantum expectation values $\langle X\rangle$. It is a particularity of the CL model that total fluctuation is recovered simply by adding up quantum and statistical fluctuations.

An example of the $\Sigma_{QQ}(t)$ evolution obtained using Eq. (24) (circles) is compared to the exact result (solid line) in Fig. 1. As an indication, the evolution of quantum fluctuation σ_{QQ}, which is identical for all trajectories, is also displayed (dotted line). Note that Eq. (16) is already exact for the evolution of first moments $\langle P\rangle$ and $\langle Q\rangle$, even if the noise is omitted. However, it completely fails to

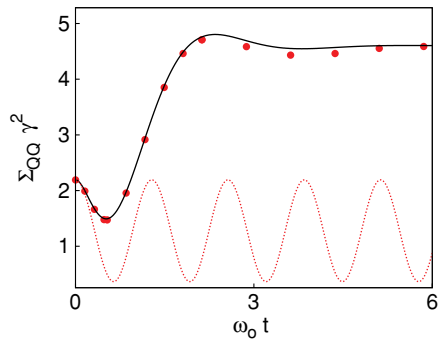

FIG. 1. (Color online) Evolution of Σ_{QQ} (circles) obtained by averaging over 10^5 trajectories. This evolution is compared to the exact result (solid line) and to the quantum fluctuation σ_{QQ} evolution (dotted line). Parameters of the simulation are $k_BT = \hbar\omega_0$, $\hbar\Omega = 5\hbar\omega_0$, $\eta = 0, 5\hbar\omega_0$, and $\hbar\omega_0 = 14$ MeV. The factor γ, defined as $\gamma^2 = \hbar/(2M\omega_0)$, equals here $\gamma = 1.216\ \mathrm{fm}^{-1}$.

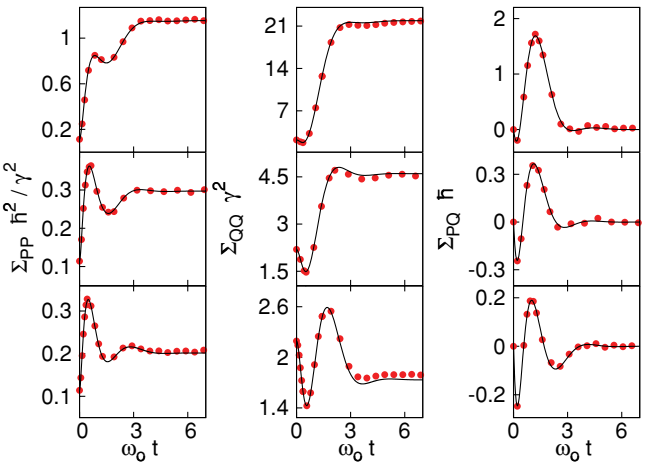

FIG. 2. (Color online) Evolution of Σ_{PP} (left), Σ_{QQ} (middle), and Σ_{PQ} (right) obtained with 10^5 trajectories, displayed with circles as a function of time and systematically compared with the exact evolution (solid line); $k_BT = 5\hbar\omega_0, \hbar\omega_0$, and $0, 1\hbar\omega_0$ are shown from top to bottom, respectively. In all cases, $\eta = 0, 5\hbar\omega_0$, $\hbar\Omega = 5\hbar\omega_0$, and $\hbar\omega_0 = 14$ MeV.

account for fluctuation. While the quantum evolution does not present any damping, the average evolution closely follows the exact solution. The harmonic oscillations in σ_{QQ} are due to the fact that the width of the initial density differs from the width of the coherent state associated with the considered oscillator, that is, $\sigma_{QQ}(0) \neq \hbar/(2M\omega_0)$. This is at variance with the simulation of Ref. [51].

The accuracy of the QMC theory has been systematically investigated for various temperatures and coupling strengths. In all cases, averaged evolutions could almost not be distinguished from the exact evolution. This is illustrated in Fig. 2, where Σ_{PP} (Fig. 2, left), Σ_{QQ} (Fig. 2, middle), and Σ_{PQ} (Fig. 2, right) are displayed as a function of time and are compared to exact solutions for various temperatures. Figure 2 clearly shows that the stochastic method properly includes all non-Markovian effects. In particular, at low temperature—typically, $k_BT < \hbar\omega_0$—and with medium coupling constant η, a large memory effect is expected.

B. Application of NZ and TCL

Jointly with the benchmark of QMC approaches, we also tested a projection method based either on the NZ [19,38,39,52] or TCL [19,40,41,52] formalism. Both theories provide a priori exact reformulations of the initial problem and lead to a closed master equation for the system density. However, they differ completely in strategy and the equation of motion used to incorporate memory effects. In the NZ case, the evolution of the system density at time t depends on its full history [i.e., on $\rho_S(s)$ for all $s \leqslant t$]. In the TCL case, the master equation is local in time, and non-Markovian effects are treated in time-dependent transport coefficients. To illustrate the differences between our new QMC method and TCL, we give, as a reminder, the corresponding local master equation for $V = Q \otimes B$:

$$\hbar\frac{d}{dt}\rho_S(t) = -i[H_S, \rho_S(t)] - \frac{i}{2}\Delta(t)[Q, \{Q, \rho_S(t)\}] - 2i\lambda(t)[Q, \{P, \rho_S(t)\}] - \frac{D_{PP}(t)}{\hbar}[Q,[Q, \rho_S(t)]] + 2\frac{D_{PQ}(t)}{\hbar}[Q, [P, \rho_S(t)]], \quad (25)$$

where $\Delta(t)$, $\lambda(t)$, $D_{PQ}(t)$, and $D_{PP}(t)$ are time-dependent transport coefficients that contain memory effects. Similarly to the QMC case, the solution of the master equation [Eq. (25)] is equivalent to following first and second moments given by

$$\begin{cases} \frac{d\langle Q\rangle}{dt} = \frac{\langle P\rangle}{M}, \\ \frac{d\langle P\rangle}{dt} = -M\omega_p^2(t)\,\langle Q\rangle - 2\lambda(t)\langle P\rangle, \\ \frac{d\Sigma_{PP}}{dt} = -2M\omega_p^2(t)\,\Sigma_{PQ} - 4\lambda(t)\Sigma_{PP} + 2D_{PP}(t), \\ \frac{d\Sigma_{QQ}}{dt} = 2\frac{\Sigma_{PQ}}{M}, \\ \frac{d\Sigma_{PQ}}{dt} = -M\omega_p^2(t)\,\Sigma_{QQ} - 2\lambda(t)\Sigma_{PQ} + \frac{\Sigma_{PP}}{M} + 2D_{PQ}(t), \end{cases}$$

with $\omega_p^2(t) = \omega_0^2 + \Delta(t)$. In practice, the exact NZ or TCL theory cannot be exactly solved, and an expansion in powers of the coupling constant is made. In the following, NZ2 (TCL2) will refer to the expansion up to second order, while NZ4 (TCL4) will refer to the expansion made up to fourth order. By neglecting higher orders in the coupling in NZ2 (TCL2) or NZ4 (TCL4), neither theory is exact anymore. In the following, the efficiency of each method is systematically discussed.

In Fig. 3, the evolution of Σ_{PP} for different cutoff frequencies $\hbar\Omega$ and coupling strengths η are compared to the exact evolution (solid line). Explicit forms of the equation of motion in the NZ and TCL cases can be found in Refs. [19,38,39,52] and Refs. [19,40,41,52], respectively. Several important remarks could be drawn from this comparison. (i) In all cases, when the coupling strength is considered up to second order, NZ2 (open triangles) provides a better approximation than TCL2 (open squares). This might indeed be expected since NZ2 and TCL2 are equivalent to the Born and Redfield master equation, respectively, and the former contains a priori less approximations than the latter. (ii) While the TCL4 (filled squares) leads to a clear improvement compared to the TCL2, NZ4 (filled triangles) is, in general, worse than NZ2. This is a known difficulty of the NZ approach and was one of the motivations for the introduction of the TCL method (see the discussion in Refs. [19,40,41]). This stems from the fact that the order in perturbation in NZ cannot be identified. For instance, NZ2 (NZ4) contains orders in coupling constant greater than 2 (4). As a result, the NZ theory does not lead to better results when the "apparent" order in the coupling increases. The TCL method essentially cures this pathology, and precise orders in the coupling can be selected. (iii) Rather large deviations between the exact and TCL2 are observed for different cutoff frequencies and coupling strengths. This issue is important because several theories have been recently developed along the line of TCL2 to include memory effects in fusion and fission reactions [14,15,17]. Note that the accuracy of TCL2 depends on different parameters used in the spectral density, in particular, the parameter $\hbar\Omega$. Here we have used a value of the cutoff frequency between 10 and 20 MeV, which

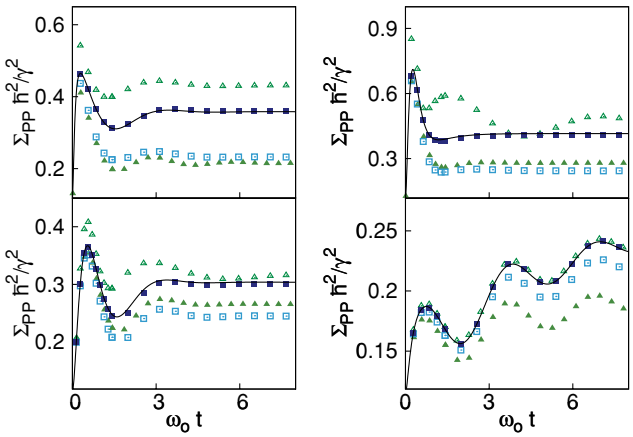

FIG. 3. (Color online) Evolution of Σ_{PP} for different approximations: NZ2 (open triangles), NZ4 (solid triangles), TCL2 (open squares), and TCL4 (solid squares). The exact evolution is displayed with a solid line. In all cases, $\hbar\omega_0 = 14$ MeV and $k_BT = \hbar\omega_0$ are used. (left) Different cutoff frequencies: (top) $\hbar\Omega = 20\hbar\omega_0$ and (bottom) $\hbar\Omega = 5\hbar\omega_0$; in both cases, $\eta = 0, 5\hbar\omega_0$. (right) $\hbar\Omega = 10\hbar\omega_0$ and different coupling strengths are used: (top) $\eta = \hbar\omega_0$ and (bottom) $\eta = 0.1\hbar\omega_0$.

gives realistic dissipation and fluctuation for the fusion or fission mechanism [14,15,18]. Our study clearly points out that a proper treatment of memory requires us to include higher order effects. (iv) Finally, in all cases, TCL4 could not be distinguished from the exact result. As we will see, the efficiency of TCL4 is similar for the inverted parabola. Because the NZ method is not competitive, only the QMC and TCL methods are considered in the following application.

C. QMC method applied to inverted oscillators

Several approaches have been recently developed to describe fusion and fission reactions [6,14,15,17,18,53]. In these mechanisms, few collective degrees of freedom couple to a sea of internal excitations while passing an inverted barrier. At very low energy, both quantum and non-Markovian effects are expected to play a significant role. Most of the theory currently used starts from quantum master equations deduced from TCL2. The QMC method offers a practical alternative that has similarities with path integral theory. Path integrals are known to provide a possible framework for including dissipation while passing barriers (see, e.g., Ref. [54]). However, owing to their complexity, only a few applications have been made so far [2,55]. We compare here the different approaches for inverted potential ($\varepsilon = -1$).

Initially, we consider a Gaussian density with quantum width $\sigma_{QQ}(0) = 0.16$ fm^2 and $\sigma_{PQ}(0) = 0$ MeV fm/c and positioned on one side of the potential (here taken arbitrarily at $\langle Q(0)\rangle = Q_0 > 0$, while the barrier height is located at 0 fm and is, by convention, taken as $V_B = 0$ MeV). The initial kinetic energy, denoted $E_K(0)$, is set by boosting the density with an initial momentum $\langle P(0)\rangle = P_0 < 0$.

Contrary to the classical theory of Brownian motion, the notion of trajectories is not so easy to tackle in the present

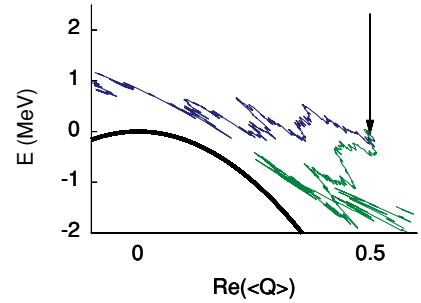

FIG. 4. (Color online) Evolution of $E(t)$ as a function of $Q(t)$ for two trajectories (dark and light lines) with $\Delta E = 0$ MeV, $k_BT = 1$ MeV, and $\eta = 0.003$ MeV. The arrow indicates the initial position of the trajectories, while the potential is also shown with a bold line for reference.

Monte Carlo framework. First, observables are complex. As mentioned in Sec. III A, this difficulty can be overcome by grouping trajectories by pairs, which is equivalent to replacing the expectations of observables by their real parts. Second, it should be kept in mind that the present theory is a purely quantum theory in which densities associated with wave packets are evolved. Therefore each trajectory should be interpreted in the statistical sense of quantum mechanics and contains many classical paths. Nevertheless, to visualize the trajectory, we define the following energies:

$$E(t) = \frac{P(t)^2}{2m} - \frac{1}{2}m\omega_0^2 Q(t)^2, \tag{26}$$

where $Q(t)$ and $P(t)$ denote the real part of $\langle Q(t)\rangle$ and $\langle P(t)\rangle$ along the trajectory. An illustration of two trajectories, one passing the barrier and one reflected, is shown in Fig. 4. As illustrated in the following, it is convenient to group trajectories according to the quantity ΔE, defined by

$$\Delta E = E(0) - V_B, \tag{27}$$

which is nothing but the difference between total initial energy and barrier height. Both trajectories shown in Fig. 4 correspond to $\Delta E = 0$ MeV.

It is tempting to group trajectories into those passing the barrier and those reflected by the potential to get information on the passing probability or passing time; however, it should be kept in mind that the present theory is fully quantal. Because each trajectory is associated with densities with quantum widths, both trajectories presented in Fig. 4 contribute to the transmission probability.

The accuracy of different methods is illustrated in Fig. 5, where evolutions of $\langle Q\rangle$, $\langle P\rangle$, Σ_{QQ}, and Σ_{PP} are shown as a function of time. Values of parameters retained for this figure are typical values generally taken in the nuclear context [16]. In all cases, including TCL2, second moments are well reproduced. However, only TCL4 and the stochastic simulation provides a correct description of first moments. Calculations are shown here for $\Delta E = 0$ MeV. TCL2 provides an increasingly better approximation when ΔE increases, while the disagreement increases below the barrier. This will be further illustrated later.

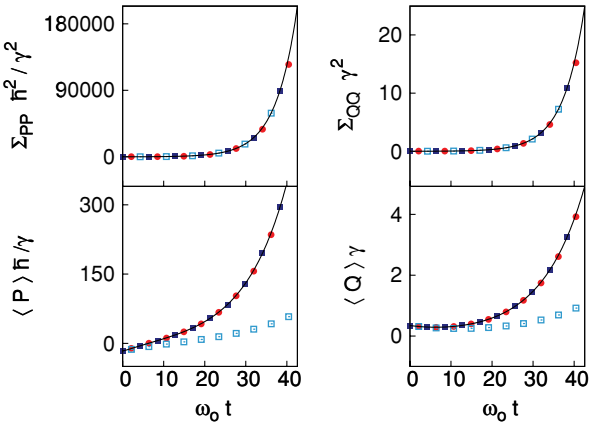

FIG. 5. (Color online) Evolution of $\langle Q\rangle$, $\langle P\rangle$, Σ_{QQ}, and Σ_{PP} as a function of time obtained with quantum Monte Carlo (circles), TCL2 (open squares), and TCL4 (solid squares). The exact evolution is also displayed with a solid line. Parameters of the simulations are $V_B = 4$ MeV, $\hbar\omega_0 = 1$ MeV, $\eta = 0.03$ MeV, $\hbar\Omega = 15\hbar\omega$, $k_BT = 1$ MeV, $\Delta E = 0$ MeV, and $\gamma = 0.402$ fm^{-1}; 10^5 trajectories have been used for the quantum Monte Carlo case.

Different coupling parameters, cutoff frequencies, and temperatures have been investigated, showing that both TCL4 and QMC are very accurate theories, leading always to results on top of the exact evolutions. It should be noted that the number of trajectories used in the stochastic approach to get small statistical errors is rather small (around 10^5), which is quite encouraging for future applications.

D. Transmission probability

The accuracy of the method used to incorporate non-Markovian effects directly affects the predicting power of the theory. This aspect is illustrated here with the passing probabilities. Such a probability is a crucial ingredient, particularly for models dedicated to the formation of very heavy elements [7,14,15,17,53,56,57], and should be precisely estimated.

The asymptotic passing probability is usually defined as

$$P(+\infty) = \lim_{t\to+\infty} \frac{1}{2}\mathrm{erfc}\left(-\frac{|q(t)|}{\sqrt{2\sigma_{qq}(t)}}\right), \qquad (28)$$

where $q(t)$ and $\sigma_{qq}(t)$ denote the expectation value and second moment of Q deduced from the considered theory, respectively. In the QMC case, these quantities identify with $\overline{\langle Q(t)\rangle}$ and $\Sigma_{QQ}(t)$, respectively. To quantify the precision of each theory, we have systematically investigated the difference between the estimated passing probability and the exact probability using the parameter $\Delta P/P$:

$$\frac{\Delta P}{P} \equiv \frac{P(+\infty) - P_{\mathrm{ex}}(+\infty)}{P_{\mathrm{ex}}(+\infty)}, \qquad (29)$$

where $P(+\infty)$ and $P_{\mathrm{ex}}(+\infty)$ denote the results of the specific calculation considered and the exact calculation, respectively. Figure 6 presents the evolution of $\Delta P/P$ as a function of ΔE obtained for different coupling strengths and temperatures for

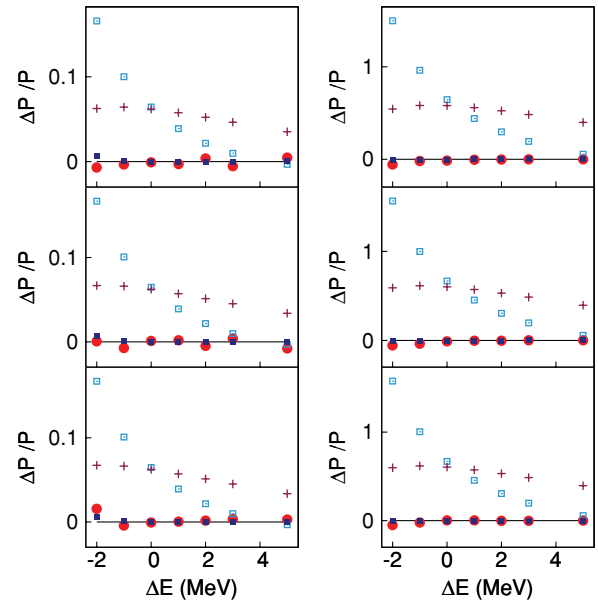

FIG. 6. (Color online) Evolution of $\Delta P/P$ as a function of ΔE calculated using quantum Monte Carlo (circles), TCL2 (open squares), TCL4 (solid squares), and Markovian approximation (crosses) for different coupling constants: (left) $\eta = 0.003$ MeV and (right) $\eta = 0.03$ MeV. In both cases, $T = 5\hbar\omega$, $\hbar\omega$, and 0, $1\hbar\omega$ are shown from top to bottom, respectively.

the QMC (circles), TCL2 (open squares), and TCL4 (solid squares) cases. In Fig. 6, the Markovian approximation is also shown by crosses.

Once again, the TCL4 and QMC methods are in perfect agreement with the exact solution for any input parameters. Small differences sometimes observed between the stochastic approach and the exact value come from the limited number of trajectories used to obtain Fig. 6. Well above the barrier (here at least two times), TCL2 converges toward the exact case. However, at low ΔE, it turns out to be a rather poor approximation. The difference seen in the TCL2 case can be traced directly back to the discrepancy already observed in Fig. 5 and further confirms the difficulty of treating non-Markovian effects below the barrier. We can see that at the lowest energy considered here, the error could be as large as 20% in the weak coupling case and more than 100% in the strong coupling limit. It is worth to mention, finally, that below the barrier, the Markovian limit gives an even better result than the TCL2 case.

IV. SUMMARY AND DISCUSSION

In this article, the QMC approach recently proposed in Ref. [43] to incorporate exactly non-Markovian effects is introduced and applied to the case of harmonic potentials coupled to a heat bath.

For both noninverted and inverted potentials, the new technique is rather effective in reproducing the exact evolution with a rather limited number of trajectories. Other methods have also been benchmarked. The TCL2 method, which is now widely used in nuclear physics to estimate passing

probabilities, turns out to deviate significantly from the expected result, especially below the barrier and even in the weak coupling regime. To properly treat the dynamics of barrier transmission, higher orders in the coupling strength should be incorporated. TCL4 gives very good agreement with the exact evolution in all cases considered here. The conclusion of our present work is that both the QMC approach and TCL4 could be considered as good candidates for including memory effects for situations of interest in nuclear physics. Henceforth, the TCL2 method, which is widely used nowadays, should be replaced by TCL4. The possibility of using stochastic formulations that are exact in average opens new perspectives in describing a system coupled to a complex environment. The application to harmonic potentials gives interesting insight into such a theory. Application to more general potentials turns out to be less straightforward, with the appearance of spikes, which have already been observed in several formalisms in which nonlinear stochastic equations appear [28]. To make these theories more versatile, new methods, such as the one proposed recently in Ref. [58], could be used.

ACKNOWLEDGMENTS

We thank D. Boilley for his careful reading of the manuscript and G. Adamian and N. Antonenko for fruitful discussions.

[1] W. U. Schröder and J. R. Huizenga, Treatise Heavy Ion Sci. **3**, 115 (1984).
[2] P. Fröbrich and R. Lipperheide, *Theory of Nuclear Reactions* (Oxford University Press, New York, 1996).
[3] J. F. Berger, M. Girod, and D. Gogny, Nucl. Phys. **A428**, 23 (1984).
[4] P. Möller and S. G. Nilsson, Phys. Lett. **B31**, 283 (1970).
[5] Y. Abe, S. Ayik, P.-G. Reinhard, and E. Suraud, Phys. Rep. **275**, 49 (1996).
[6] Y. Aritomo, T. Wada, M. Ohta, and Y. Abe, Phys. Rev. C **59**, 796 (1999).
[7] Y. Abe, D. Boilley, B. G. Giraud, and T. Wada, Phys. Rev. E **61**, 1125 (2000).
[8] Y. Abe, Eur. Phys. J. A **13**, 143 (2002).
[9] C. Shen, G. Kosenko, and Y. Abe, Phys. Rev. C **66**, 061602(R) (2002).
[10] A. Diaz-Torres, D. J. Hinde, M. Dasgupta, G. J. Milburn, and J. A. Tostevin, Phys. Rev. C **78**, 064604 (2008).
[11] D. Boilley and Y. Lallouet, J. Stat. Phys. **125**, 473 (2006).
[12] S. Matsumoto and M. Yoshimura, Phys. Rev. A **63**, 012104 (2000).
[13] C. Rummel and H. Hofmann, Nucl. Phys. **A727**, 24 (2003).
[14] N. Takigawa, S. Ayik, K. Washiyama, and S. Kimura, Phys. Rev. C **69**, 054605 (2004).
[15] S. Ayik, B. Yilmaz, A. Gokalp, O. Yilmaz, and N. Takigawa, Phys. Rev. C **71**, 054611 (2005).
[16] V. Sargsyan, Y. Palchikov, Z. Kanokov, G. Adamian, and N. Antonenko, Physica A **386**, 36 (2007).
[17] K. Washiyama, N. Takigawa, and S. Ayik, in *Symposium on Nuclear Physics VI, AIP Conference Proceedings* (New York, 2007), vol. 891, p. 413.
[18] V. V. Sargsyan, Z. Kanokov, G. G. Adamian, and N. V. Antonenko, Phys. Rev. C **77**, 024607 (2008).
[19] H. Breuer and F. Petruccione, *The Theory of Open Quantum Systems* (Oxford University Press, Oxford, 2002).
[20] M. B. Plenio and P. L. Knight, Rev. Mod. Phys. **70**, 101 (1998).
[21] J. T. Stockburger and H. Grabert, Phys. Rev. Lett. **88**, 170407 (2002).
[22] J. Dalibard, Y. Castin, and K. Mølmer, Phys. Rev. Lett. **68**, 580 (1992).
[23] R. Dum, P. Zoller, and H. Ritsch, Phys. Rev. A **45**, 4879 (1992).
[24] N. Gisin and I. Percival, J. Phys. A **25**, 5677 (1992).
[25] H. Carmichael, *An Open Systems Approach to Quantum Optics* (Springer, Berlin, 1993).
[26] Y. Castin and K. Mølmer, Phys. Rev. A **54**, 5275 (1996).
[27] M. Rigo and N. Gisin, Quantum Semiclass. Opt. **8**, 255 (1996).
[28] W. Gardiner and P. Zoller, *Quantum Noise* (Springer, Berlin, 2000).
[29] W. T. Strunz, Phys. Lett. **A224**, 25 (1996).
[30] L. Diósi, N. Gisin, and W. T. Strunz, Phys. Rev. A **58**, 1699 (1998).
[31] W. T. Strunz, L. Diósi, and N. Gisin, Phys. Rev. Lett. **82**, 1801 (1999).
[32] W. T. Strunz, New J. Phys. **7**, 91 (2005).
[33] J. Piilo, S. Maniscalco, K. Härkönen, and K.-A. Suominen, Phys. Rev. Lett. **100**, 180402 (2008).
[34] J. Shao, J. Chem. Phys. **120**, 5053 (2004).
[35] D. Lacroix, Phys. Rev. A **72**, 013805 (2005).
[36] D. Lacroix and G. Hupin, in *FUSION08: New Aspects of Heavy Ion Collisions near the Coulomb Barrier, AIP Conference Proceedings* (New York, 2008), vol. 1098, pp. 128–132.
[37] A. O. Caldeira and A. J. Leggett, Ann. Phys. **149**, 374 (1983).
[38] S. Nakajima, Prog. Theor. Phys. **20**, 948 (1958).
[39] R. Zwanzig, J. Chem. Phys. **33**, 1338 (1960).
[40] F. Hashitsume, N. Shibata, and M. Shingū, J. Stat. Phys. **17**, 155 (1977).
[41] F. Shibata, Y. Takahashi, and N. Hashitsume, J. Stat. Phys. **17**, 171 (1977).
[42] H.-P. Breuer, Eur. Phys. J. D **29**, 105 (2004).
[43] D. Lacroix, Phys. Rev. E **77**, 041126 (2008).
[44] H.-P. Breuer, D. Burgarth, and F. Petruccione, Phys. Rev. B **70**, 045323 (2004).
[45] H.-P. Breuer, Phys. Rev. A **69**, 022115 (2004).
[46] Y. Zhou, Y. Yan, and J. Shao, Eur. Phys. Lett. **72**, 334 (2005).
[47] H.-P. Breuer and F. Petruccione, Phys. Rev. E **76**, 016701 (2007).
[48] W. Gardiner, *Handbook of Stochastic Methods* (Springer, Berlin, 1985).
[49] R. P. Feynman and F. L. Vernon, Ann. Phys. **24**, 118 (1963).
[50] A. J. Leggett, S. Chakravarty, A. T. Dorsey, M. P. A. Fisher, A. Garg, and W. Zwerger, Rev. Mod. Phys. **59**, 1 (1987).
[51] J. T. Stockburger and H. Grabert, Chem. Phys. **268**, 249 (2001).
[52] J. Gemmer and H.-P. Breuer, Eur. Phys. J. ST **151**, 1 (2007).
[53] D. Boilley, Y. Abe, and J. Bao, Eur. Phys. J. A **18**, 627 (2003).
[54] A. O. Caldeira and A. J. Leggett, Phys. Rev. Lett. **46**, 211 (1981).
[55] P. Fröbrich, R. Lipperheide, and K. Möhring, Z. Phys. B **78**, 325 (1990).
[56] J.-D. Bao and D. Boilley, Nucl. Phys. **A707**, 47 (2002).
[57] B. Yilmaz, S. Ayik, Y. Abe, and D. Boilley, Phys. Rev. E **77**, 011121 (2008).
[58] W. Koch, F. Großmann, J. T. Stockburger, and J. Ankerhold, Phys. Rev. Lett. **100**, 230402 (2008).